

Determining trace metal speciation in soils at molecular-scale by combined X-ray fluorescence, diffraction and absorption

A. Manceau^{1,2}, N. Tamura¹, R.S. Celestre¹, A.A. MacDowell¹, G. Sposito², H.A. Padmore¹

¹ Advanced Light Source, Lawrence Berkeley National Laboratory, Berkeley, California 94720, USA

² *Environmental Geochemistry Group, Hilgard Hall, University of California, Berkeley, CA 94720, USA*

INTRODUCTION

Understanding how environmentally-important trace metals are sequestered in soils at the molecular scale is critical to developing a solid scientific basis for maintaining soil quality and formulating effective strategies to remediate severely contaminated areas. The speciation of Zn and Ni in flood plain soils was determined by a novel synergistic use of three non-invasive synchrotron-based techniques, X-ray microfluorescence (μ SXRF); X-ray microdiffraction (μ XRD); and extended X-ray absorption fine structure spectroscopy (EXAFS). Eight nodules from the Mississippi basin were examined by μ SXRF and μ XRD on the 7.3.3. microdiffraction beamline, and complementary EXAFS measurements were performed at the European Synchrotron Radiation Facility in Grenoble (France). Here, only the first set of results is presented.

RESULTS AND INTERPRETATION

The chemical composition of the nodules was determined using inductively coupled plasma atomic emission spectroscopy (ICP-AES) and inductively coupled plasma mass spectroscopy (ICP-MS). These analyses gave [Fe] = 57526 (σ = 21213), [Mn] = 25592 (σ = 17716), [Zn] = 76 (σ = 51), [Ni] = 67 (σ = 21) mg/kg. The σ variability of the bulk analyses is relatively low, and contrasts with the μ SXRF maps, which show that individual nodules are highly heterogeneous at the micrometer scale, containing distinct areas of concentrated Fe, Mn, Ni and Zn (Fig. 1).

The mineralogy and crystal chemistry of Zn and Ni in the series of nodules is completely represented by the three samples in Fig. 1. Nodule 1 shows, on average, little correlation between Fe and Mn ($r_{\text{Fe-Mn}}$ = 0.62), but visual inspection of the maps shows that the degree of correlation varies laterally. The richest Fe areas in the outer region are strongly depleted in Mn, whereas the inner region contains areas of both high Mn and high Fe. Zn and Ni are strongly correlated with Fe ($r_{\text{Fe-Zn}}$ = 0.84, $r_{\text{Fe-Ni}}$ = 0.88) and, to a lesser extent, with Mn ($r_{\text{Mn-Zn}}$ = 0.71, $r_{\text{Mn-Ni}}$ = 0.78). The relatively high $r_{\text{Mn-Ni}}$ value does not necessarily indicate that a Ni fraction is actually associated with Mn, but instead can result from the incomplete separation of Fe and Mn in the core of a nodule. μ XRD patterns were collected with a CCD camera at different points selected on the elemental maps. The outermost Fe-rich region was found to consist of finely-dispersed goethite (α -FeOOH). Quartz, feldspar, titanium oxide, and carbonate grains also were detected. The Fe-Mn core consists of either Mn-feroxyhite (δ -FeOOH) or Fe-vernadite (δ -MnO₂), depending on the Fe/Mn ratio. Therefore, Zn and Ni appear to be predominantly bound to goethite in this nodule.

Mn, Fe, Zn, and Ni were also unevenly distributed in nodule 2 (Fig. 1b), which showed a moderate overall correlation between Fe and Mn ($r_{\text{Fe-Mn}}$ = 0.78). However, the central region is high in Fe and Mn, whereas the external Fe layer is depleted in Mn. As with the previous nodule, this result illustrates the spurious meaning of elemental correlations calculated solely from total chemical analyses. Nodule 2 possesses a Zn-Ni “hot spot”, about 80 x 80 μm^2 in area, which is strongly

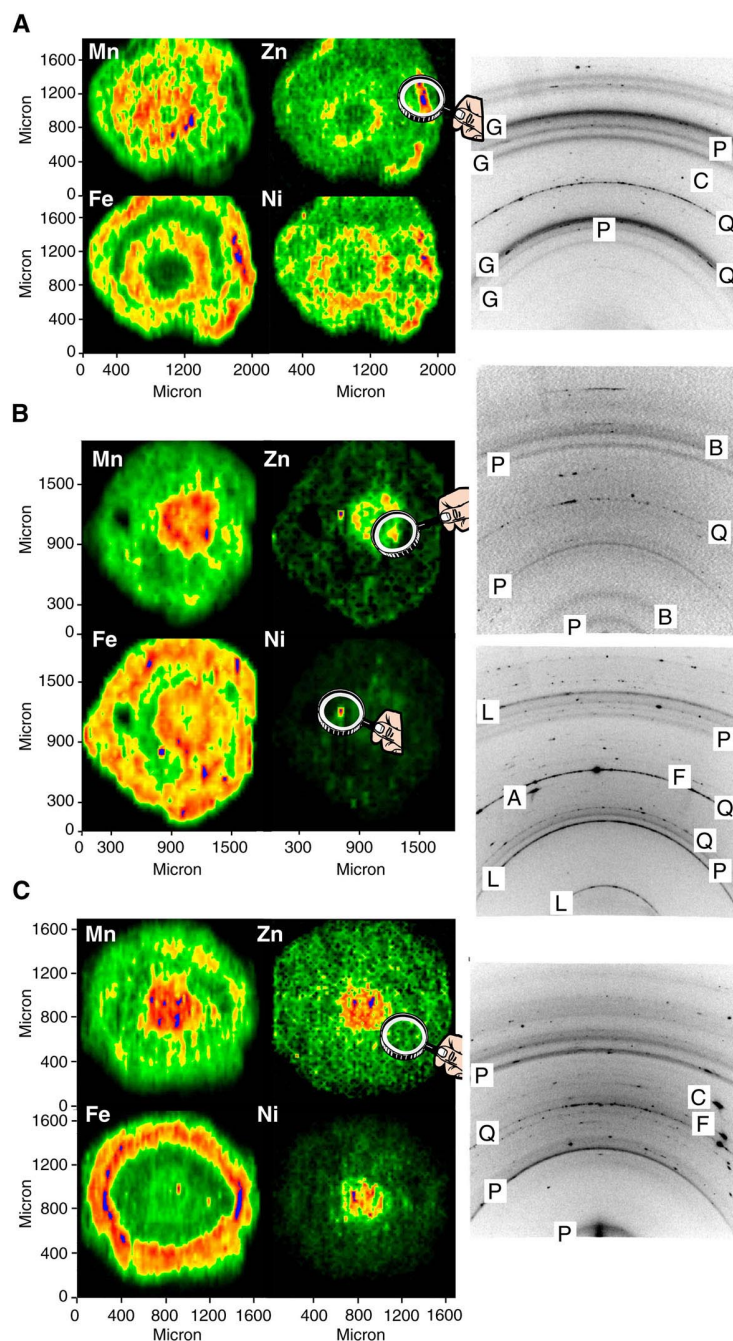


Figure 1. Synchrotron-based micro-X-ray fluorescence (μ SXRF) maps obtained by scanning soil nodules under a monochromatic beam ($E = 10$ keV; beam size on the sample: $10 \mu\text{m H} \times 25 \mu\text{m V}$; step size: $32 \times 32 \mu\text{m}$ (a), $42 \times 42 \mu\text{m}$ (b), $25 \times 25 \mu\text{m}$ (c); counting time: 5 to 8 s/point). μ XRD patterns were collected at selected points of interest using a 1024×1024 pixels CCD camera and an exposure time of 10 to 20 min ($E = 6.0$ keV (a, b) and 6.3 keV (c)). All data were collected in reflection geometry mode by inclining the sample at $6^\circ \theta$. B = hexagonal birnessite (main diffraction peaks at 7.1 – 7.2 \AA , 2.45 \AA , and 1.41 \AA), G = goethite (main diffraction peaks at 4.18 \AA and 2.69 \AA), L = lithiophorite (main diffraction peaks at 9.4 \AA , 4.7 \AA , and 2.37 \AA), P = phyllosilicate (main diffraction peaks at 4.45 – 4.48 \AA , 2.55 – 2.58 \AA , and 1.50 \AA). In (a) Ni and Zn are associated with goethite (α -FeOOH); in (b) Ni is associated with lithiophorite, and Zn with lithiophorite and birnessite; in (c) Ni is associated with lithiophorite and Zn with lithiophorite and phyllosilicate.

correlated with Mn. The core of the nodule is enriched in Zn as well, but devoid of Ni, suggesting that nodule 2 contains two major Zn species, but only a single Ni species, one which also contains Zn. The mineralogical nature of the minute Mn grain containing both Zn and Ni was identified by μ XRD as lithiophorite, a MnO_2 - $\text{Al}(\text{OH})_3$ mixed-layer phyllosilicate (Fig. 2). In the two-dimensional XRD pattern, Bragg reflections from this grain formed a continuous Debye ring, characteristic of a powder diffraction pattern. The lithiophorite is, therefore, very fine-grained like most natural reactive particles. Randomly-layered birnessite (also termed vernadite), together with phyllosilicate, was positively identified in the central region by μ XRD (Fig. 1b). Vernadite and lithiophorite are considered to be the two predominant Mn mineral species in near-surface environments, but their defective structure (vernadite) and small particle size pose major problems for identifying them by conventional XRD. The combination of μ SXRF and μ XRD provides the necessary lateral resolution for establishing their presence and role in the sequestration of trace metals.

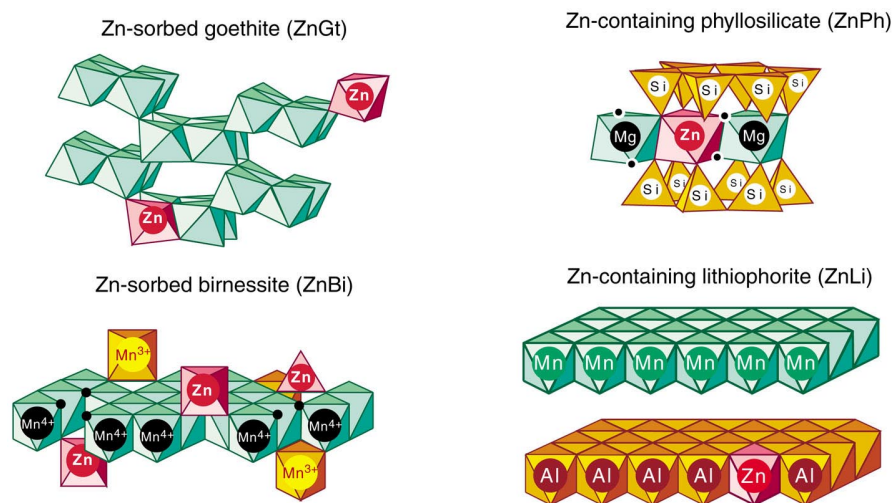


Figure 2. Structure of minerals in which Zn and Ni are sequestered.

Two Zn fractions were also detected in nodule 3 (Fig. 1c). In the first, Zn is concentrated with Ni and Mn at the core, which, according to μ XRD, contains lithiophorite and phyllosilicate, a geochemical association already found in nodule 2. The second fraction of Zn has a uniform background signal distributed throughout the nodule and likely as well in the central region, where it is masked by the Zn,Ni lithiophorite species. Clearly, this second Zn fraction is not bound either to Fe or Mn oxides, because neither the Fe nor the Mn map shows areal contours similar to the Zn map. μ XRD patterns collected in Zn-containing (but Fe- and Mn-depleted) regions showed the presence of dioctahedral phyllosilicates (Fig. 1c). Therefore, the second Zn fraction likely corresponds to a Zn-containing phyllosilicate. It was almost impossible to find regions containing only Fe or Mn oxides. For example, the four two-dimensional μ XRD patterns presented in Fig. 1 all contain diffraction rings at 4.45-4.48 Å and 2.55-2.58 Å, typical of the 020-110 and 130-200 reflections that characterize sheet silicates. A peak at 1.50 Å was observed systematically at higher diffraction angles, thus indicating the mostly dioctahedral structure of these minerals. Elemental correlation coefficients for nodule 3 can be interpreted readily based on these results. Little correlation was obtained for Fe and Mn ($r_{\text{Fe-Mn}}=0.69$), in agreement with the nonoverlapping contour maps for these two elements. The Mn-Zn correlation is moderate ($r_{\text{Mn-Zn}}=0.76$) owing to

the partial association of Zn with phyllosilicate, whereas the Mn-Ni correlation is strong ($r_{\text{Mn-Ni}}=0.82$) since Ni is uniquely bound to lithiophorite. Correlations between Fe and Zn ($r_{\text{Fe-Zn}}=0.44$) or Fe- and Ni ($r_{\text{Fe-Ni}}=0.33$) are low, as expected.

In summary, μSXRF and μXRD microanalyses showed that Zn is bound to four mineral species, goethite, phyllosilicate, hexagonal birnessite, and lithiophorite, whereas nickel is sequestered by goethite and lithiophorite. This difference in speciation of Zn and Ni provides a clue to the observed higher partitioning of Ni in the soil nodules over the soil matrix. Nodules commonly form in soils with restricted internal drainage by the solubilisation of Fe(II) and Mn(II) under reducing conditions, followed by precipitation as Fe(III) and Mn(III,IV) oxides under oxidising conditions. Consequently, concretions have the same quantities of phyllosilicates and coarse grains (quartz, feldspar, titanium oxides...) as does the soil matrix, but they contain a higher quantity of finely-divided Fe and Mn oxides that cement soil material together and reduce its porosity. Since Zn is predominantly speciated as a phyllosilicate (EXAFS data not shown), and because this latter mineral is uniformly present in the soil, Zn partitioning in nodules is necessarily limited. The high Ni partitioning into the nodules results directly from selective sequestration by Fe and Mn oxides, the principal minerals that cause nodule formation. Thus, the novel combination of μSXRF , μXRD , and EXAFS spectroscopy provides the approach needed to speciate metals in a natural matrix not possible to study accurately with conventional techniques.

This work was supported by the LBNL Laboratory Director's Research and Development Fund and by the US Department of Energy, Office of Basic Energy Sciences, under contract # DOE-AC03-76SF00098.

Principal investigator: Alain Manceau, Advanced Light Source, Ernest Orlando Lawrence Berkeley National Laboratory. Email: amanceau@lbl.gov. Telephone: 510-643-2324.